

Leveraging High Resolution Spectra to Understand Black Hole Spectra

Michael A. Nowak^{1,*}

Massachusetts Institute of Technology, Kavli Institute for Astrophysics, Cambridge, MA 02139, USA

Received 9 October 2016, accepted 1 December 2016

Published online later

Key words accretion, accretion disks — stars: black holes — X-rays: binaries — X-rays: individual (Cygnus X-1)

For the past 17 years, both *XMM-Newton* and *Chandra* have brought the powerful combination of high spatial and spectral resolution to the study of black hole systems. Each of these attributes requires special consideration— in comparison to lower spatial resolution, CCD quality spectra— when modeling observations obtained by these spacecraft. A good understanding of the high resolution spectra is in fact required to model properly lower resolution CCD spectra, with the Reflection Grating Spectrometer (*RGS*) instrument on *XMM-Newton* maintaining the highest “figure of merit” at soft X-ray energies for all missions flying or currently planned for the next decade. Thanks to its even higher spectral resolution, the use of *Chandra*-High Energy Transmission Gratings (*HETG*), albeit with longer integration times, allows for one to bring further clarity to *RGS* studies. A further promising route for continued studies is the combination of high spectral resolution at soft X-rays, via *RGS* and/or *HETG*, with contemporaneous broadband coverage extending to hard X-rays (e.g., *NuSTAR* or *INTEGRAL* spectra). Such studies offer special promise for answering fundamental questions about accretion in black hole systems; however, they have received only moderate consideration to date. This may be due in part to the difficulty of analyzing high resolution spectra. In response, we must continue to develop software tools that make the analysis of high resolution X-ray spectra more accessible to the wider astrophysics community.

© 2017 WILEY-VCH Verlag GmbH & Co. KGaA, Weinheim

1 Introduction

Fundamental questions remain in the study of astrophysical black holes. What are the most robust techniques for measuring black hole spin? (See the reviews of Middleton 2016; Reynolds & Nowak 2003.) How does this spin relate to the formation of jets in these systems? (See Fender & Muñoz-Darias 2016.) What are the relationships between jets and outflowing winds, and how much mass and accretion energy is transported by the latter? (See Ponti et al. 2012.) What fraction of the hard X-rays can be explained by jet emission, and what fraction can be attributed to a corona? (See Markoff et al. 2015.) Does the disk recede as black holes transit from high/soft states to low/hard states? (See the review by Done et al. 2007.) Answers to these questions have been sought via multi-wavelength observations ranging from radio wavelengths through hard X-ray energies, as many of the above cited phenomena manifest themselves over broad energy bands.

The soft X-ray, however, holds special importance for a number of components. It is where the disk spectrum peaks. It is crucial for studies of wind properties. It dominates the bolometric luminosity in Galactic black hole “high states”. Arguably, the two most important instruments for study of the soft X-ray spectra of black hole systems have been the *XMM-Newton* and *Chandra* satellites. Both of these instruments share the properties of having unparalleled spatial and spectral resolution. The latter is achieved via the Reflec-

tion Gratings Spectrometer (*RGS*; den Herder et al. 2001) of *XMM-Newton*, and by the Low Energy Transmission Gratings (*LETG*; Brinkman et al. 2000) and High Energy Transmission Gratings (*HETG*; Canizares et al. 2005) of *Chandra*. The *HETG* is comprised of the High Energy Gratings (*HEG*) and Medium Energy Gratings (*MEG*). Both the high spatial and spectral resolution properties of these instruments pose unique challenges that are often overlooked in analyses of black hole systems. The high spectral resolution properties especially have not been utilized as often as they should or could be in multi-wavelength campaigns.

We present examples below from both stellar mass and supermassive black holes. We briefly discuss the synergy between *RGS* and *HETG* high spectroscopic resolution studies. We then discuss the state of software for high resolution spectroscopic analysis. We end with considerations of the current use of high resolution spectra in multi-satellite, broadband X-ray campaigns.

2 Low/High Resolution Comparisons

As a first example, Fig. 1 shows a spectrum of the black hole candidate (BHC) and X-ray binary, Cyg X-1. The observation occurred at orbital phase 0 (superior conjunction), when the optical companion was directly between our line of sight to the black hole. This particular observation was quasi-simultaneous in *all X-ray satellites flying at that time* (April 2006), with the *Chandra-HETG* and *Suzaku* spectra previously being discussed in Nowak et al. (2011). There

* Corresponding author: e-mail: mnowak@space.mit.edu

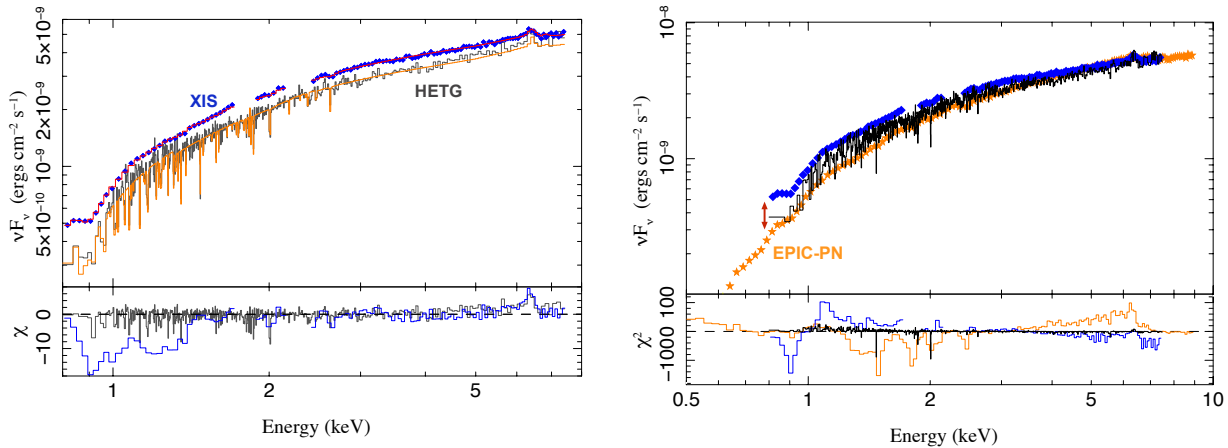


Fig. 1 Left: Comparison of quasi-simultaneous flux-corrected *Suzaku*-XIS (blue diamonds) and *Chandra*-HETG (grey histogram) spectra of a hard state of Cyg X-1. (Times of dips, see below, have been excluded.) The model (red and orange histograms, respectively) consists of a disk, powerlaw, and Fe K α emission line absorbed by both neutral and ionized emission. Scattering of the soft X-ray photons out of the line of sight by a foreground dust halo is included in the HETG, but not *Suzaku*, fit. Residuals (histogram colors match their respective data colors) show the fit absent both the Fe K α emission and ionized absorption (Nowak et al. 2011). Right: the same spectra as on the left, now with the addition of quasi-simultaneous EPIC-PN spectra (orange stars), fit with an absorbed and dust-scattered (*Chandra*-HETG and EPIC-PN only) powerlaw (model not shown), with cross normalizations set so that the spectra match at 7 keV.

are a number of issues that arose in analyzing these spectra. First is the effect of spatial resolution in *XMM-Newton* and *Chandra*. To a first approximation, the presence of foreground dust scatters soft X-rays out of the arcsec scale field of view of these instruments, but X-rays scatter back in (albeit time-delayed) on the arcminute scale field of view of instruments such as *Suzaku*. This effect is noticed on the right side of Fig. 1, where the “flux-corrected” spectra from EPIC-PN and HETG lie below that of *Suzaku*. This is *not* (or at least not predominantly) a calibration effect, but is instead due to dust scattering that had to be included in the modeling on the left portion of Fig. 1. This effect is described in more detail for various X-ray instruments by Corrales et al. (2016).

A recent *Chandra*/*Swift* study of the black hole candidate V404 Cyg by Heinz et al. (2016) shows that observations of black holes with long-term time variations can probe the location and composition of dust in the interstellar medium (ISM). *XMM-Newton* is perhaps the current best instrument to perform such observations going forward, as it has the proper combination of high (enough) spatial resolution with large effective area in the soft X-rays, yet is relatively free of pileup (see Davis 2001) compared to *Chandra*.

The second effect noticeable in Fig. 1 is the presence of ionized absorption, clearly visible in the *Chandra*-HETG spectra, yet completely unresolved but *extremely statistically significant* in the *Suzaku* and EPIC-PN spectra (Nowak et al. 2011). It is important to note that both the ionized absorption, as well as prominent dipping events that occur as a function of orbital phase in Cyg X-1, are associated with absorption by a powerful wind from the O star secondary in this system (see the discussions and references in Hanke et al. 2009; Mišková et al. 2016). The

spectra shown here *occur outside of all detectable dipping events at phase 0*. Such ionized absorption, only spectroscopically resolvable by RGS, LETG, and HETG spectra, is a ubiquitous feature in spectra of Cyg X-1 (Mišková et al. 2016). This is demonstrated in the right most figure of Fig. 2, where the relative amplitude of this component is shown as a function of orbital phase in *non-dip* *Suzaku* spectra of Cyg X-1.

Fig. 2 shows color-color diagrams from the full *Suzaku* and *Chandra* observations associated with Fig. 1. The extension to the lower left (excluded in the shown spectra) is due to the interspersal of dense clumps passing in front of our line of sight during the observations. The “tail” from the lower left to the lower right, however, is due to the “partial covering” nature of these clumps. In *Suzaku*, this is also an artifact of the dust scattering halo, as we are seeing the time-delayed scattering from foreground halos on arcminute scales, with the fitted covering fraction being consistent with the fraction of flux scattered by dust (Nowak et al. 2011). Such scales are resolved out by the *Chandra* point spread function (PSF); however, there remains an $\approx 2\%$ uncovered fraction. Although this may be due to the inner core of the dust halo, another possibility is that it is due to partial covering in time. That is, we might be seeing large dipping events passing through our line of sight on time scales faster than the ≈ 1.8 s integration times of these *Chandra* observations. Exploring this possibility, however, would require the larger effective area and faster timing capabilities of *XMM*.

This latter experiment potentially has been conducted with the recent (Summer 2016) observations of Cyg X-1 conducted by *XMM-Newton*, which were designed (PI: P. Uttley) to conduct spectral-timing studies of the continuum, Fe band, and reflection spectra of Cyg X-1, as well as

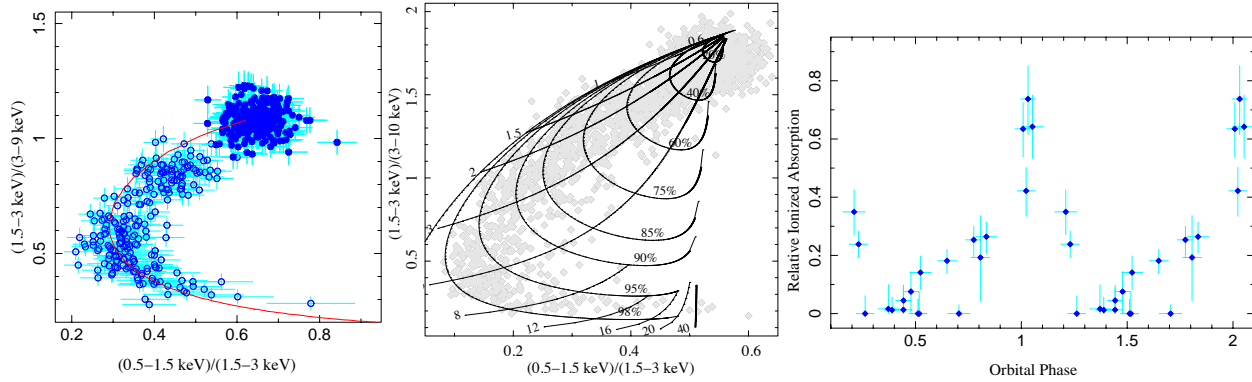


Fig. 2 Left: Color-color diagram of the full *Suzaku* observation of Cyg X-1, from Fig. 1, now including dipping events. The red line is a simple partial covering model that describes these events with a varying column, but fixed partial covering fraction (Nowak et al. 2011). Middle: Color-color diagram derived from *Chandra-HETG* data of Cyg X-1, including dipping events. Lines show simple partial covering models as on the left, with covering fractions ranging from 20–98% and columns ranging over $(0.6\text{--}40)\times 10^{22}\text{ cm}^{-2}$. (See the discussions in Hanke et al. 2009.) Right: Relative degree of ionized absorption in *Suzaku* observations of Cyg X-1 hard states, compared to that found in the orbital phase 0 (superior conjunction) observation of Fig. 1. All of these fits are for *times without any dipping events*.

to perform high-resolution absorption spectroscopy of the secondary wind. It is important to note here that *XMM-Newton-RGS* is ideally suited for such studies as it has the highest “figure of merit” for soft X-ray band spectroscopy, as shown in Fig. 3. *This would still be true below $\approx 0.8\text{ keV}$, even if the Hitomi mission had not been lost.* The power of this *RGS* capability can be seen in Fig. 3 where two (non-simultaneous, but very comparable in terms of flux, spectral shape, and integration time) observations of the same BHC are shown, highlighting *MEG* and *RGS* spectra of the oxygen absorption edge region. Among potential future studies to be considered with *RGS* are detailed spectral-temporal observations of galactic black hole systems, especially over binary orbits, to separate out absorption components local to the system from those due to the ISM.

The advantage of galactic binary BHC studies, aside from spectral signal-to-noise, are the time scales involved. In Cyg X-1, thanks to high resolution spectroscopy from *RGS* and *HETG*, we know that both ionized absorption and “partial covering” models are applicable. We can track their changes over binary orbits, and thus have the strong promise of separating out their effects from those associated with the inner accretion flow, e.g., the relativistically broadened Fe $K\alpha$ line. Such effects are more difficult, but no less important, to disentangle with high resolution spectroscopic observations of Active Galactic Nuclei (AGN). This is directly relevant to studies of relativistic features in AGN, where some researchers have suggested that what is modeled as a broadened line is in fact due to features dominated by partial covering (Miller et al. 2009). For the case of NGC 3783, Brenneman et al. (2011) showed the necessity of simultaneously fitting the warm absorption and broad line features. Further work by Reynolds et al. (2012) showed how the model parameter regions of Miller et al. (2009) and Brenneman et al. (2011) are related, with the latter being fa-

vored in Markov Chain Monte Carlo (MCMC) analyses of the spectra. Also important in the work of Brenneman et al. (2011) and Reynolds et al. (2012) was the inclusion of hard X-ray spectra, which we discuss further below.

3 *XMM-Newton/Chandra Synergies*

The figure of merit presented in Fig 3 tells only part of the story; absolute spectral resolution is still an important metric. For the absorption edge of 4U 1957+11 shown in Fig. 3, the higher effective area of the *RGS* as compared to the *MEG* clearly greatly benefits our ability to model these features. Here, however, the edge and its associated absorption lines (i.e., transitions of atomic oxygen; see Juett et al. 2004), as well as the possible ionized features from either the interstellar medium (see Yao & Wang 2005) or the local system (Nowak et al. 2008), are well-isolated. This is not always the case, especially with absorption features in the soft X-ray band covered by the *RGS*.

As an example in Fig. 4 we show a portion of an *RGS* spectrum of the Seyfert galaxy PG1211+143, from the work of Pounds et al. (2016a,b) (see also Pounds et al. 2017, in this volume). Based upon both prior *EPIC-PN* studies (Pounds et al. 2003) and these more recent *RGS* studies, it has been argued that PG1211+143 exhibits blueshifted, ionized outflows moving at speeds in the galaxy rest frame of $\mathcal{O}(10\%)$ the speed of light. The best evidence, however, is that there are *multiple* ionized components at a variety of outflow velocities that are blended in the *RGS* spectra (Pounds et al. 2016a,b). Furthermore, basic line properties, such as line widths, are not resolved by the *RGS* spectra. Clearly separating ionized outflow components and resolving their individual line widths requires the resolution of the *Chandra-HETG*; however, such observations require large investments of observing time.

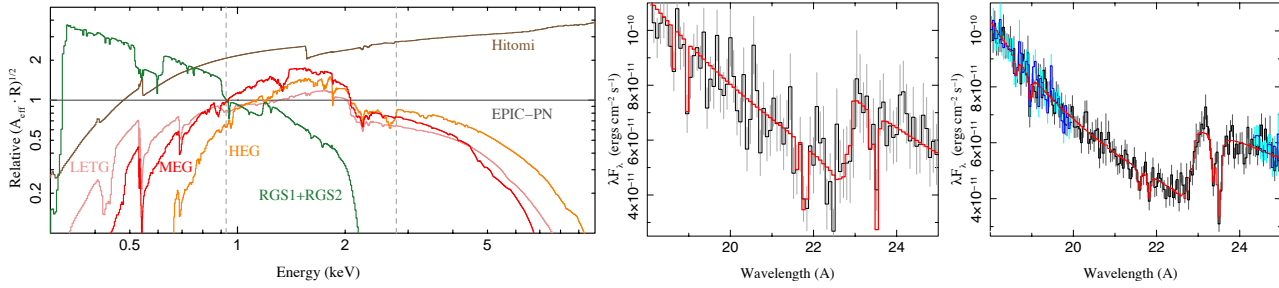


Fig. 3 Left: Figure of merit for emission and absorption line studies (square root of effective area times spectral resolution) for various instruments, normalized to that for *EPIC-PN*. The vertical dashed lines show the energies below which *Chandra-HEG* (right) and *XMM-Newton-RGS* (left) spectral resolution exceeds that achieved by the *Hitomi* calorimeter. Middle/Right: Comparison of two comparable (in terms of flux, spectral shape, and exposure time) *HETG* (middle) and *RGS* (right) observations of the oxygen-edge region of the black hole candidate 4U 1957+11 (see Nowak et al. 2012). The spectrum is a multi-color disk with peak temperature ≈ 1.7 keV absorbed by a neutral column of $1.2 \times 10^{21} \text{ cm}^{-2}$. There is also evidence for ionized absorption by the warm phase of the interstellar medium, as well as by material local to the system.

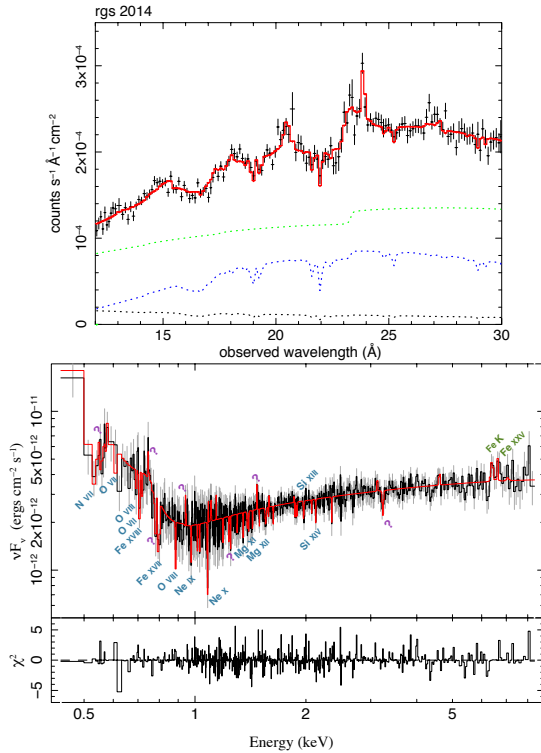


Fig. 4 Top: *XMM-Newton-RGS* spectra of the Seyfert galaxy PG1211+143 (figure from Pounds et al. 2016b; see also Pounds et al. 2016a), fit with an absorbed continuum and several ionized outflow components. Bottom: *Chandra-HETG* spectrum of PG1211+143 (Danekhar et al. 2016, in prep.). The figure is labeled with possible lines, found from a blind search, consistent with an outflowing wind at a single (galaxy restframe) blueshift. Question marks are potential lines also found in the blind search that have not yet been identified with absorption or emission components.

To this end, we have obtained an *HETG* observation (PI: Julia Lee) of PG1211+143 for a total integration time of 450 ks. Fig. 4 shows the binned, combined *HETG* spectra, with “blind search” line fits (Danekhar et al. 2016, in prep.) derived from the unbinned spectra. This figure further shows possible line identifications for a set of features at a common blueshift of $0.06c$, consistent with one of the outflows described by Pounds et al. (2016a). The full analysis will be described elsewhere by Danekhar et al. (2016); however, we note that the analysis heavily draws upon the higher effective area, albeit lower resolution, *RGS* analysis. It likely would have been impossible to obtain the *HETG* observations for this integration time, or have found these features in even a blind search in shorter *HETG* observations, without first having the preliminary studies with *XMM-Newton-RGS*.

A further example of this synergy between *XMM-Newton-RGS* and *Chandra-HETG* is shown in Fig. 5, where we show a simulation of an upcoming 500 ks *HETG* observation of NGC 1313 X-1. Analysis of archival *RGS* observations suggests ionized emission at systemic velocities, as well as ionized absorption at both systemic and blueshifted outflow ($v \approx 0.1c$) velocities (Pinto et al. 2016). These components, however, are unresolved by the *RGS*, but would have taken significant integration times to discover with *HETG* observations alone. Based upon the initial *RGS* studies, a commitment was made to use 500 ks (out of an annual allocation of 700 ks to *HETG* PI Claude Canizares) of *HETG* Guaranteed Time Observations (GTO). The goals of these observations will be to resolve line widths and to obtain more precise outflow velocity measurements. Comparing the simulations shown in Fig. 5 to Fig. 3, we see that much of the *HETG* gains will come from the 1–2 keV region where its figure of merit exceeds that of *RGS*. We see again, however, the utility of having first used the higher effective area *RGS* to identify a high resolution spectroscopy target of interest. Furthermore, the *RGS* observations allowed us to determine a plau-

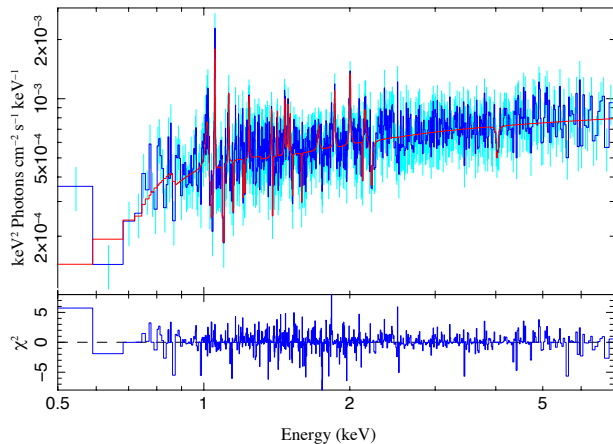


Fig. 5 Simulated 500 ksec *Chandra-HETG* spectrum of the ULX NGC 1313 X-1, based upon ionized absorption and emission line fits of *RGS* spectra presented by Pinto et al. (2016) (see their Fig. 1). The model fit corresponds to a “blind line search” implemented in *ISIS* (Houck & Denicola 2000) (see §4), and recovers many of the features from the input model.

sible, albeit significant, *HETG* integration time for follow-up study.

4 Line Analysis Software

A difficulty in the analysis of high resolution X-ray spectra is the complexity of models required to describe the data. Above ≈ 3 keV, e.g., the Fe region, where spectral lines are relatively few and widely spaced, simple direct modeling of individual line features may be feasible. In the soft X-ray bands covered by the *RGS*, *LETG*, and *MEG*, lines can be numerous and closely spaced, complicating the analysis. Few codes exist for describing emission and absorption by the photoionized plasmas relevant to the study of black hole systems, among them are *CLOUDY*, (Ferland et al. 1998, 2013), *XSTAR* (Kallman & Bautista 2001), and the models included in the *SPEX* analysis package (Kaastra et al. 1996). These codes take a global approach to description of the high resolution spectra, modeling multiple individual lines and blends simultaneously. As such, however, searching parameter space can be slow and unintuitive, and the codes and code results can be difficult to interpret. E.g., for the lines that comprise the best fit, identification of individual components, and obtaining access to the relevant atomic data that led to those components, can be difficult. Creating custom interfaces to these codes can be cumbersome, especially in cases where the source code is not publicly available (e.g., *SPEX*). These issues can lead to a “potential barrier”, discouraging the use of high resolution X-ray spectra.

To further reduce the barrier to entry to the study of high resolution X-ray spectra, a number of researchers have been creating more user-friendly tools for both fitting and

interpreting such models. Graphical user interfaces to the atomic databases for piecewise fits to restricted wavelength regions are being explored. (See the individual talks by T. Kallman and R. Smith at the 2016 meeting¹ of the International Astronomical Consortium for High Energy Calibration [IACHEC]). *XSTARDB* is a code suite for use within *ISIS* that provides easier access to the *XSTAR* atomic data (e.g., individual line identifications, line searches based on transition strengths, etc.), that also manages and runs *XSTAR* spectral fits.

In the example of PG1211+143 above, we have employed an *ISIS* script suite that we are developing that allows for more phenomenological analysis of high resolution data. (Preliminary code versions are available as part of the *ISIS* scripts maintained and developed at Remis Observatory².) The scripts allow for modeling of individual lines using a choice of standard profiles (e.g., gaussian or Voigt profiles, with parameters input in energy or wavelength, with or without explicit redshift parameters). Lines are added to the model parameter file either in wavelength or energy order, with users being able to name the line profile (e.g., a redshifted gaussian added as a description of Fe $K\alpha$ could be named `zg_FeKa`). For Fig. 4, the lines were placed in a multiplicative model (to allow them to describe either emission or absorption lines, with the latter never formally describing negative counts), with their names enumerating the statistical order in which they were added in a blind line search. (E.g., the most significant line, likely from NeX, was called `zg_0`, while the seventh most significant line, likely from NeIX, was called `zg_6`.)

We plan to expand this code to allow for the easy addition of multiple levels of functional ties, such as tying redshifts across profiles expected to come from similar temperature/ionization states, while simultaneously tying line strengths within a line series. The scripts will include procedures for applying blind line searches to the data. The goal is to allow a preliminary, straightforward phenomenological description of the spectra as a prior step before embarking upon more physical descriptions with, for example, complex and slow running photoionization codes.

5 Summary

As discussed above, high resolution spectra provide unique information about black hole systems. Looking forward to future observations with *XMM-Newton-RGS* and *Chandra-HETG*, one important area that we must consider is broadband, multi-satellite observations. For the example of NGC 3783, as shown by Brenneman et al. (2011) and Reynolds et al. (2012), both high resolution, soft X-ray spectra and broadband (in that case, *Suzaku*; going forward in the future, most likely utilizing *NuSTAR*) are necessary to understand relativistic features. Indeed, García et al.

¹ web.mit.edu/iachec/meetings/2016/

² www.sternwarte.uni-erlangen.de/isis/

(2015) has recently shown that under ideal circumstance, given knowledge of the underlying continuum and quality observations, the soft X-ray reflection spectrum *measures* the cutoff at high energies. In practice, however, concerns about ionized absorption, as discussed in Nowak et al. (2011) for the case of Cyg X-1, must first be addressed with, e.g. high spectral resolution observations. Clearly, however, just as there is a synergy between CCD and gratings quality spectra (§2), and a synergy between large effective area *RGS* spectra and higher resolution *HETG* spectra (§3), there is also a synergy between soft X-ray and hard X-ray spectroscopy.

It is somewhat unfortunate, then, that this avenue has not yet been strongly explored. Although there have been many successful simultaneous *XMM-Newton* and *NuSTAR* observations, an examination of the literature to date shows that of the approximately 100 papers describing *XMM-Newton/NuSTAR* observations, only 11 discuss *RGS* spectra in any capacity. Of the dozen accepted joint *Chandra/NuSTAR* proposals, only three utilize the *HETG*. (One of these campaigns is a joint observation of NGC 3783; PI L. Brenneman.)

When sufficient telemetry exists, and instrumental constraints aren't violated, *RGS* spectra will always be obtained with an *XMM-Newton* observation. This does not necessarily guarantee that the *RGS* will have sufficient signal-to-noise for use, but in many cases it does. How do we encourage users to analyze these data? We note that the work of Pinto et al. (2016) was derived from archival observations from proposals that were initially designed to obtain CCD-quality spectra. How do we encourage users to explicitly design programs around the use of *RGS* spectra?

For *Chandra* proposals, gratings observations (typically dominated by the use of *HETG*) comprise only $\approx 15\%$ of the accepted program. This is not because gratings proposals are accepted at a lower rate than non-gratings proposals, rather it is because they represent only 15% of the submitted proposals. How do we encourage users to apply for more gratings observations?

Part of the issue is undoubtedly the complexity of the spectra, and the lack of an “easy entry” to the high resolution spectroscopy software (§4). The high resolution spectroscopy community must continue to develop tools that allow for wider use of existing and future data. Examples—such as those in Fig. 1 or the case of NGC 3783 and similar AGN—where CCD-quality spectra cannot be properly analyzed without knowledge of the high resolution spectra must also be emphasized.

As shown in Fig. 3, *RGS* below ≈ 0.9 keV and *HETG* between ≈ 0.9 –2 keV are the premiere instruments for spectroscopic studies. A relaunch of a satellite comparable to *Hitomi* would not alter the situation for *RGS*. High resolution spectroscopy has the capability of providing measures of density, temperatures, and velocities, and is in fact the prime scientific mission of the proposed *Athena* and *X-ray Surveyor* missions. Continued studies with *RGS*,

LETG, and *HETG* must pave the way for these future missions.

Acknowledgements. Michael Nowak gratefully acknowledges funding support from the National Aeronautics and Space Administration through the Smithsonian Astrophysical Observatory contract SV3-73016 to MIT for support of the *Chandra* X-ray Center, which is operated by the Smithsonian Astrophysical Observatory for and on behalf of the National Aeronautics Space Administration under contract NAS8-03060. He further acknowledges support by NASA Grant NNX12AE37G. He would like to thank V. Grinberg, D. Huenemoerder, M. Middleton, and J. Wilms for useful conversations.

References

- Brenneman, L. W., Reynolds, C. S., Nowak, M. A., et al. 2011, *ApJ*, 736, 103
- Brinkman, B. C., Gunsing, T., Kaastra, J. S., et al. 2000, in *Society of Photo-Optical Instrumentation Engineers (SPIE) Conference Series*, ed. J. E. Truemper & B. Aschenbach, Vol. 4012, Society of Photo-Optical Instrumentation Engineers (SPIE) Conference Series, 81
- Canizares, C. R., Davis, J. E., Dewey, D., et al. 2005, *PASP*, 117, 1144
- Corrales, L. R., García, J., Wilms, J., & Baganoff, F. 2016, *MNRAS*, 458, 1345
- Davis, J. E., 2001, *ApJ*, 562, 575
- den Herder, J. W., Brinkman, A. C., Kahn, S. M., et al. 2001, *A&A*, 365, L7
- Done, C., Gierliński, M., & Kubota, A. 2007, *ARA&A*, 15, 1
- Fender, R., & Muñoz-Darias, T. 2016, in *Lecture Notes in Physics*, Berlin Springer Verlag, ed. F. Haardt, V. Gorini, U. Moschella, A. Treves, M. Colpi, Vol. 905, *Lecture Notes in Physics*, Berlin Springer Verlag, 65
- Ferland, G. J., Korista, K. T., Verner, D. A., et al. 1998, *PASP*, 110, 761
- Ferland, G. J., Porter, R. L., van Hoof, P. A. M., et al. 2013, *Revista Mexicana de Astronomía y Astrofísica*, 49, 137
- García, J. A., Dauser, T., Steiner, J. F., et al. 2015, *ApJ*, 808, L37
- Hanke, M., Wilms, J., Nowak, M. A., et al. 2009, *ApJ*, 690, 330
- Heinz, S., Corrales, L., Smith, R., et al. 2016, *ApJ*, 825, 15
- Houck, J. C., & Denicola, L. A. 2000, in *ASP Conf. Ser. 216: Astronomical Data Analysis Software and Systems IX*, Vol. 9, 591
- Juett, A. M., Schulz, N. S., & Chakrabarty, D. 2004, *ApJ*, 612, 308
- Kaastra, J. S., Mewe, R., & Nieuwenhuijzen, H. 1996, in *UV and X-ray Spectroscopy of Astrophysical and Laboratory Plasmas*, ed. K. Yamashita, T. Watanabe, 411
- Kallman, T., & Bautista, M. 2001, *ApJS*, 133, 221
- Markoff, S., Nowak, M. A., Gallo, E., et al. 2015, *ApJ*, 812, L25
- Middleton, M., 2016, in *Astrophysics of Black Holes: From Fundamental Aspects to Latest Developments*, ed. C. Bambi, Vol. 440, *Astrophysics and Space Science Library*, 99
- Miller, L., Turner, T. J., & Reeves, J. N. 2009, *MNRAS*, 399, L69
- Miškovičová, I., Hell, N., Hanke, M., et al. 2016, *A&A*, 590, A114
- Nowak, M. A., Hanke, M., Trowbridge, S. N., et al. 2011, *ApJ*, 728, 13
- Nowak, M. A., Juett, A., Homan, J., et al. 2008, *ApJ*, 689, 1199
- Nowak, M. A., Wilms, J., Pottschmidt, K., et al. 2012, *ApJ*, 744, 107
- Pinto, C., Middleton, M. J., & Fabian, A. C. 2016, *Nature*, 533, 64
- Ponti, G., Fender, R. P., Begelman, M. C., et al. 2012, *MNRAS*, L417
- Pounds, K., Lobban, A., Reeves, J., & Vaughan, S. 2016a, *MNRAS*, 457, 2951
- Pounds, K. A., Lobban, A., Reeves, J. N., Vaughan, S., & Costa, M. 2016b, *MNRAS*, 459, 4389
- Pounds, K. A., Reeves, J. N., King, A. R., O'Brien, P. T., & Turner, M. J. L. 2003, *MNRAS*, 345, 705
- Reynolds, C. S., Brenneman, L. W., Lohfink, A. M., et al. 2012, *ApJ*, 755, 88
- Reynolds, C. S., & Nowak, M. A. 2003, *Physics Reports*, 377, 389
- Yao, Y., & Wang, Q. D. 2005, *ApJ*, 624, 751